Tectonophysics 491 (2010) 85–95

Contents lists available at ScienceDirect

Tectonophysics

journal homepage: www.elsevier.com/locate/tecto

Comparison of fault models of the 2008 Wenchuan earthquake (Ms8.0) and spatial distributions of co-seismic deformations

Wuxing Wang [a,b,*], Wenke Sun [b,c], Zaisen Jiang [b]

[a] Laboratory of Computational Geodynamics, Graduate University of Chinese Academy of Sciences, Beijing, China
[b] Institute of Earthquake Science, China Earthquake Administration, Beijing, China
[c] Earthquake Research Institute, University of Tokyo, Tokyo, Japan

ARTICLE INFO

Article history:
Received 11 February 2009
Received in revised form 23 June 2009
Accepted 31 August 2009
Available online 10 September 2009

Keywords:
2008 Wenchuan earthquake
Slip distribution
Fault model
Co-seismic deformation
Earth model

ABSTRACT

A proper slip fault model and a reasonable dislocation theory are necessary to compute and investigate co-seismic deformations caused by the 2008 Wenchuan earthquake (Ms8.0). To find such a model, several comparisons are made of different dislocation theories, seismic fault models, and earth models. Results indicate that the fault model determined by combining GPS and seismic waveform data is the best. The spherical dislocation theory yields better results than that of a half-space theory, and the results obtained from a revised PREM earth model are better than those from PREM. According to results of earlier investigations, co-seismic deformations such as the displacement, geoid, gravity, and strain changes caused by the 2008 Wenchuan earthquake (Ms8.0) are computed, described, and discussed. Results show that the earthquake generated considerable co-seismic deformation in a large area around the epicenter. The modeled deformations are applicable as a reference for other researchers to study inter-structural inversion, crustal deformation, etc. The effects of the curvature and layer structure are great. Moreover, spherical dislocation theory is necessary for studying co-seismic deformations caused by a large event.

1. Introduction

The tragic 2008 Wenchuan earthquake (Ms8.0), which occurred on May 12, is the latest of a series of earthquakes in the earthquake-prone Tibetan region. The earthquake occurred in an area that is deforming because of the collision of two tectonic plates that has continued now for 50 Ma: the Indian plate and the Eurasian plate. This collision has created the high mountains and widespread seismicity observed throughout central Asia. The area between India and Asia covers a wide region that is undergoing large strain and deformation, thereby engendering the Wenchuan earthquake. Fig. 1 (left) portrays the location of the 2008 Wenchuan earthquake (31.0°N, 103.4°E). The blue star represents the location of the main quake. The earthquake occurred where the Indian plate, forced further eastward, overrides the Sichuan Basin at a rate of about 4 mm/year. This is the cause of the ongoing rise of the Longmen Shan mountain range, which marks Tibet's eastern border. The motion of the landmasses, as shown in the figure, is sensed at GPS stations of the region (Wang et al., 2001). Seismological measurements indicate that the 2008 Sichuan earthquake reached a magnitude of about Ms8.0, rupturing the Longmen Shan central fault. The rupture of the fault started in Wenchuan northwest of Chengdu and then traveled about 300 km northeastward along the front of the mountain range. The source depth is about 14 km below the surface. Aftershocks occur mainly along and near the fault line ruptured by the original May 12 quake, distributed in the middle-northern fault from Yingxiu to Qingchuan (Zhang et al., 2008a). Field geological investigations have detected two surface ruptures: 240 km along the Yingxiu–Beichuan fault, and 70 km along the Guanxian–Jiangyou fault, with maximum vertical and horizontal displacements of 6 m and 4.7 m, respectively (Xu et al., 2008; Zhang et al., 2008a).

To model the seismic fault model, several investigators have presented different slip distributions (fault models), using seismic waveform data, or seismic waveforms plus GPS-observed displacements, such as those by Ji and Hayes (2008), Zhang et al. (2008b), and Wang et al. (2008). The three slip models are fundamentally similar in terms of size and seismic moment, but with vastly different details. A comparison among the three models should be made to choose the best one for interpreting observed geodetic and geophysical data, and for studying the co-seismic deformations. For this purpose, as a judgment standard, we use the GPS determined co-seismic displacements observed before and after the quake. Fig. 1 (right) depicts the positions of GPS stations at which measurements were taken after the earthquake, including three classes: the red stars represent the continuous GPS stations; the blue stars denote the regional basic GPS stations; and yellow stars show C class GPS stations, which belong to national control network. In the following sections, we introduce more details about the slip models and GPS displacements.

* Corresponding author. Laboratory of Computational Geodynamics, Graduate University of Chinese Academy of Sciences, Beijing, China.
E-mail address: bkwwx@seis.ac.cn (W. Wang).

0040-1951/$ – see front matter © 2009 Elsevier B.V. All rights reserved.
doi:10.1016/j.tecto.2009.08.035

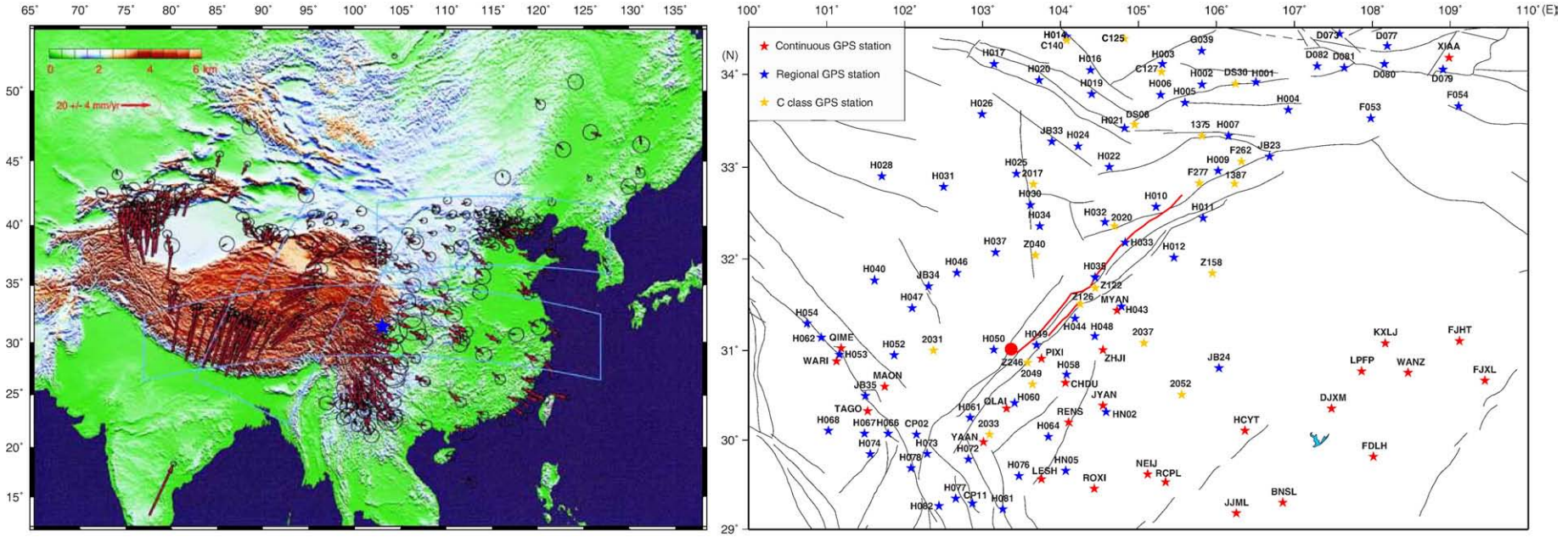

Fig. 1. (left) Location of the 2008 Sichuan earthquake (blue star) with velocity background from GPS data (Wang et al., 2001). (right) GPS observation stations where measurements were conducted after the earthquake (from Zhang et al., 2008a).

To compute proper co-seismic deformations, or invert seismic fault models, a reasonable dislocation theory should be adopted. Many scientists (Steketee, 1958; Maruyama, 1964; Press, 1965; Okada, 1985, etc.) have studied surface displacement, tilt, and strain attributable to dislocations buried in a semi-infinite medium. They have developed theoretical formulations to describe deformation of an isotropic homogeneous Earth model caused by various dislocations. Okubo (1991, 1992) examined the problem of potential and acceleration changes caused by point dislocations and by faulting on a finite plane in a homogeneous half-space. All of the studies described above presupposed a homogeneous half-space or a homogeneous nongravitating sphere. For a more realistic Earth model, e.g., the PREM model (Dziewonski and Anderson, 1981), Pollitz (1997) solved the problem of regional displacement and strain fields induced by a dislocation in a viscoelastic, non-self-gravitating model. Sun and Okubo (1993) studied the surface potential and gravity changes caused by dislocations in spherically symmetrical Earth models. Their results showed that the Earth's sphericity can cause a 10% difference when the epicentral distance is greater than 10°; radial heterogeneity should be considered when the epicentral distance is greater than 0.5°. Piersanti et al. (1995) and Sabadini et al. (1995) studied the gravity, displacement and rates induced by a dislocation in viscoelastic stratified Earth models, accounting for sphericity and self-gravitation using a self-consistent approach. They produced results of surface displacement and velocities in the near-field and far-field for various viscosity profiles in the mantle. Tanaka et al. (2006) studied the same problem using a new method that overcomes some previous numerical difficulties and guarantees accuracy. Fu and Sun (2008) presented a new theory for computing co-seismic gravity changes in a three-dimensional inhomogeneous earth model.

In this report, we first summarize the three seismic fault models described above in Section 2. Subsequently, we introduce the GPS-observed co-seismic displacements in Section 3. Following are comparisons between the observed and computed co-seismic displacements using the dislocation theories of Okada (1985) and Sun et al. (1996, 2009) to find the best slip distribution model and dislocation theory.

Then, the best slip distribution model and dislocation theory (Sun and Okubo, 1993; Sun et al., 1996, 2006, 2009) are used to calculate the co-seismic deformations such as the displacement, geoid, gravity, and strain changes caused by the 2008 Wenchuan earthquake (Ms8.0). Results show that the earthquake generated considerable co-seismic deformations in western China. They can serve as a reference for other researchers to study inter-structural inversion, crustal deformation, and other applications. Although several reports in the relevant literature (e.g., Sun and Okubo, 2002) have described effects of spherical curvature and layer structure of the Earth obtained through theoretical investigation, this large seismic event provides a good opportunity to observe those effects practically. Results show that the effects are large and that a spherical dislocation theory is necessary for studying co-seismic deformations caused by a large event.

2. Slip distributions (fault models) of the 2008 Wenchuan earthquake (Ms8.0)

Immediately after the occurrence of the earthquake, Ji and Hayes (2008) used GSN broadband waveforms downloaded from the NEIC data center, and analyzed 17 teleseismic broadband P waveforms, 10 broadband SH waveforms, and 30 long-period surface waves to obtain a preliminary slip distribution of the earthquake, which had a magnitude of Mw7.9 (Fig. 2a). The finite fault model is given by 21×8 sub-faults (15 km × 15 km cell size) with strike angle of 229° and dip angle of 33°. Using a similar method and global seismic waveform data, Zhang et al. (2008b) derived a different slip model (Fig. 2b). This fault model comprises 31×5 sub-faults (20 km × 10 km cell size), with a strike angle of 225° and a dip angle of 39°. The two slip distributions (Fig. 2a and b) portray vastly different distribution patterns. The Ji and Hayes (2008) model indicates two maximum slip areas on two sides of the fault with a maximum slip magnitude of about 9 m, whereas the Zhang et al. (2008b) model shows one maximum slip area at the earth's surface with a maximum slip magnitude of 7 m. The difference is considered to result from their different data selection criteria and data number used in the fault inversion. This fact implies that a fault model derived from seismic waveforms incorporates great uncertainty. According to Fu and Sun (2004), different slip distributions engender different distribution patterns of co-seismic deformations.

In addition to the seismic waveform data based on the geologic investigation and field surface rupture measurement, Wang et al. (2008) presented a more realistic finite fault model composed of three pieces of sub-faults, and reconstructed the source rupture process by combining teleseismic waveforms and local co-seismic displacements observed at 37 GPS stations (Fig. 2c). The Longmen Shan main fault (308 km × 40 km) is divided into 110 sub-faults with cell size of 14 km × 8 km. The front Longmen Shan fault (84 km × 32 km) comprises 24 sub-faults with cell size of 14 km × 8 km. Results show that the Wenchuan earthquake indicates thrust motion with right lateral strike slip also, and two faults (Yingxiu–Beichuan fault and Guanxian–Jiangyou fault) participated simultaneously during the rupture process. The estimated maximum slip on the fault reaches up to 12.5 m, and the slip distribution on the faults with high magnitude can be projected to Yingxiu and Beichuan, which were severely damaged.

Fig. 2 depicts that many different fault models exist for the unique seismic event. Among them, there must be only one model holding the truth. Then a natural question is which model in Fig. 2 is the best one to fit the geodetic observations. To answer this question, in Section 4, we will compare the computed displacements based on the three models with GPS data, using different dislocation theories.

3. Observed co-seismic displacements

Soon after the Wenchuan earthquake (M8.0) occurred on May 12, 2008, as a national project, Chinese scientists performed geodetic and geophysical observations using GPS and gravity and obtained valuable geodetic data (Zhang et al., 2008a). Based on the GPS data, Fig. 3 depicts the observed co-seismic horizontal displacements at 122 stations and vertical components at 44 stations. The displacement vector is denoted in red and blue, showing different scales for both horizontal and vertical displacement components. Fig. 3a portrays that the two sides of the fault principally move in opposite directions, i.e., shrinking horizontally, reflecting a thrust fault movement. The nearer the point to the fault, the greater the displacement is. In the southern area, the fault movement fundamentally shows a dip-slip pattern; the north fault area exhibits a distribution pattern with mixed dip-slip and right-strike-slip components. The vertical displacements in Fig. 3b reflect a large-scale sinking in the Sichuan Basin side. Because of the lack of observation data, it is difficult to identify the movement direction in the mountain area side. These GPS observation provide invaluable data in the inverting fault model, interpreting other geodetic and geophysical data. In the following section, these observed displacements are compared with computed ones to assess the quality of fault models.

4. Comparisons of fault models, earth models, and dislocation theories

In this section, using the two dislocation theories for two earth models, we compute co-seismic displacements for the three fault models described above. Through comparison of the modeled results with the observed displacements, we might judge and determine a

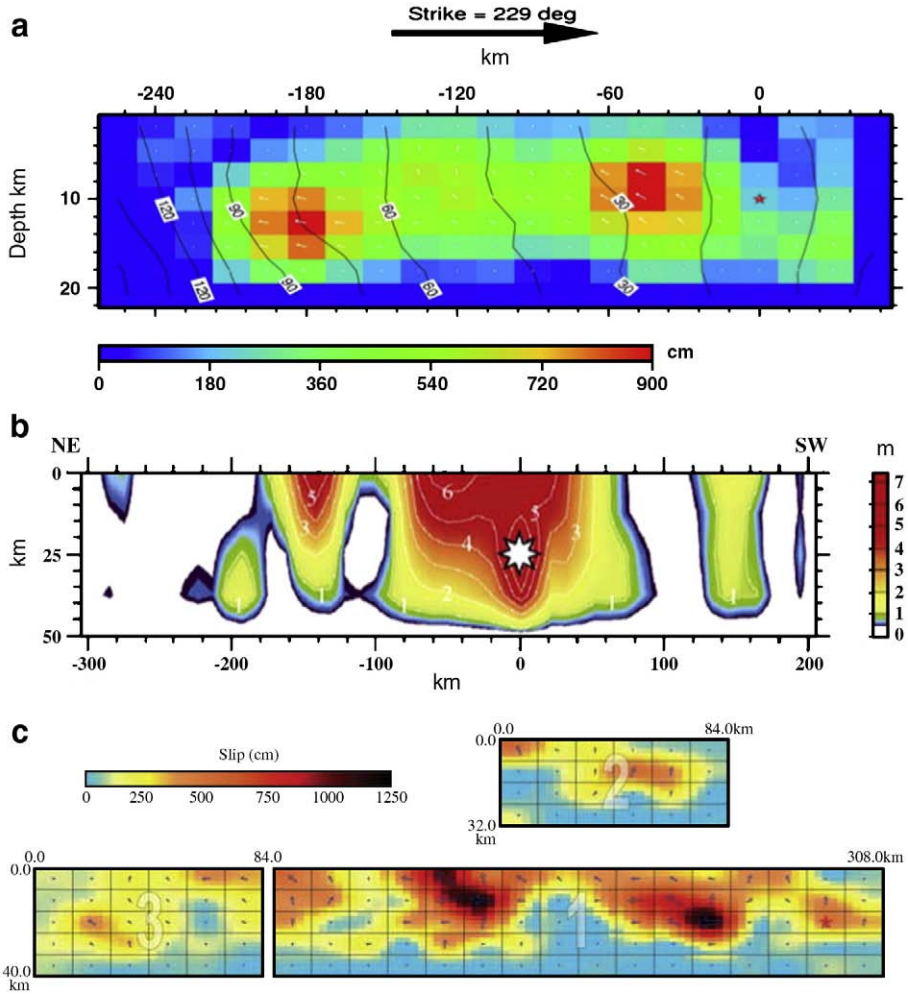

Fig. 2. Slip distributions of the 2008 Wenchuan earthquake according to (a) Ji and Hayes (2008), (b) Zhang et al. (2008a,b), and (c) Wang et al. (2008).

better fault model (slip distribution), a proper dislocation theory, and a suitable earth model.

As described above, the dislocation theories used here are those of half-space (Okada, 1985) and spherical (Sun et al., 1996, 2009) earth models. The purpose is to observe which theory best fits the observations, and which should be used in a real application. It is expected that the spherical dislocation theory is better than that of the half-space theory because the effects of spherical curvature and layered structure of the earth are incorporated in the former, but not in the latter. This conclusion is confirmed below.

Regarding the earth model, we adopt the PREM model (Dziewonski and Anderson, 1981). Actually, the original PREM model includes a liquid layer on the top surface. When it is applied to study solid earth problem, the top liquid layer is usually replaced by a solid layer beneath the liquid layer. Then the density and two elastic parameters (Lamé constants) of the top layer become $\rho = 2.6$ g/cm^3,

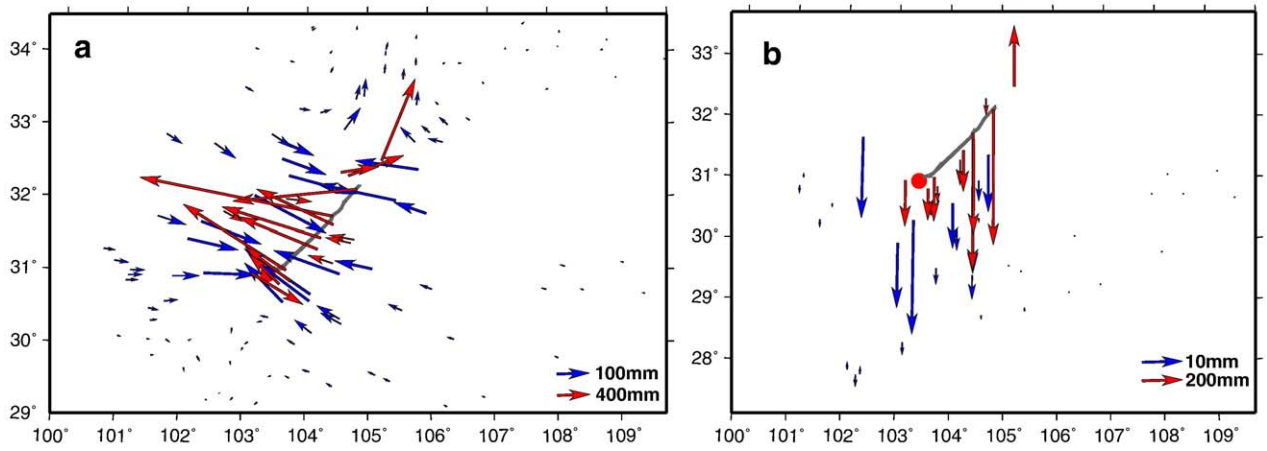

Fig. 3. Co-seismic displacements caused by the 2008 Wenchuan earthquake (Ms8.0), respectively observed at 122 GPS stations for horizontal component (a) and 44 GPS stations for the vertical component (b) (plotted based on Zhang et al., 2008a).

$\lambda = 5.20 \times 10^{11}$ dyn/cm^2, and $\mu = 2.66 \times 10^{11}$ dyn/cm^2. This model with a new top layer replaced is still called the PREM model. The corresponding Poisson's ratio is $\nu = 0.33$. To observe the effect of a different earth model, we also consider a revised PREM (called RPREM) model with parameters of $\rho = 2.9$ g/cm^3, $\lambda = 7.53 \times 10^{11}$ dyn/cm^2, and $\mu = 4.41 \times 10^{11}$ dyn/cm^2. The corresponding Poisson ratio is $\nu = 0.32$. The PREM and RPREM earth models are used for the spherical dislocation theory; the corresponding Poisson's ratios $\nu = 0.33$ and $\nu = 0.32$ are used for the half-space theory.

Then we calculate the co-seismic displacements resulting from the 2008 Wenchuan earthquake (Ms8.0), and respectively plot the results in Figs. 4 and 5 for horizontal and vertical components. To save space, Figs. 4 and 5 present results only for the RPREM model (those for PREM are omitted) because results show that the RPREM model gives better results than PREM. Comparison of the calculated displacements in Figs. 4 and 5 with the observed ones in Fig. 3 shows that the results calculated for the Wang et al. (2008) fault model (c_1 and c_2) fit the observed ones best: much better than the other two fault models. The result implies that the fault model constrained by local geodetic observations is better than that obtained solely from seismic waveform data. Furthermore, comparison of the results calculated using the half-space theory and the spherical theory indicates that the

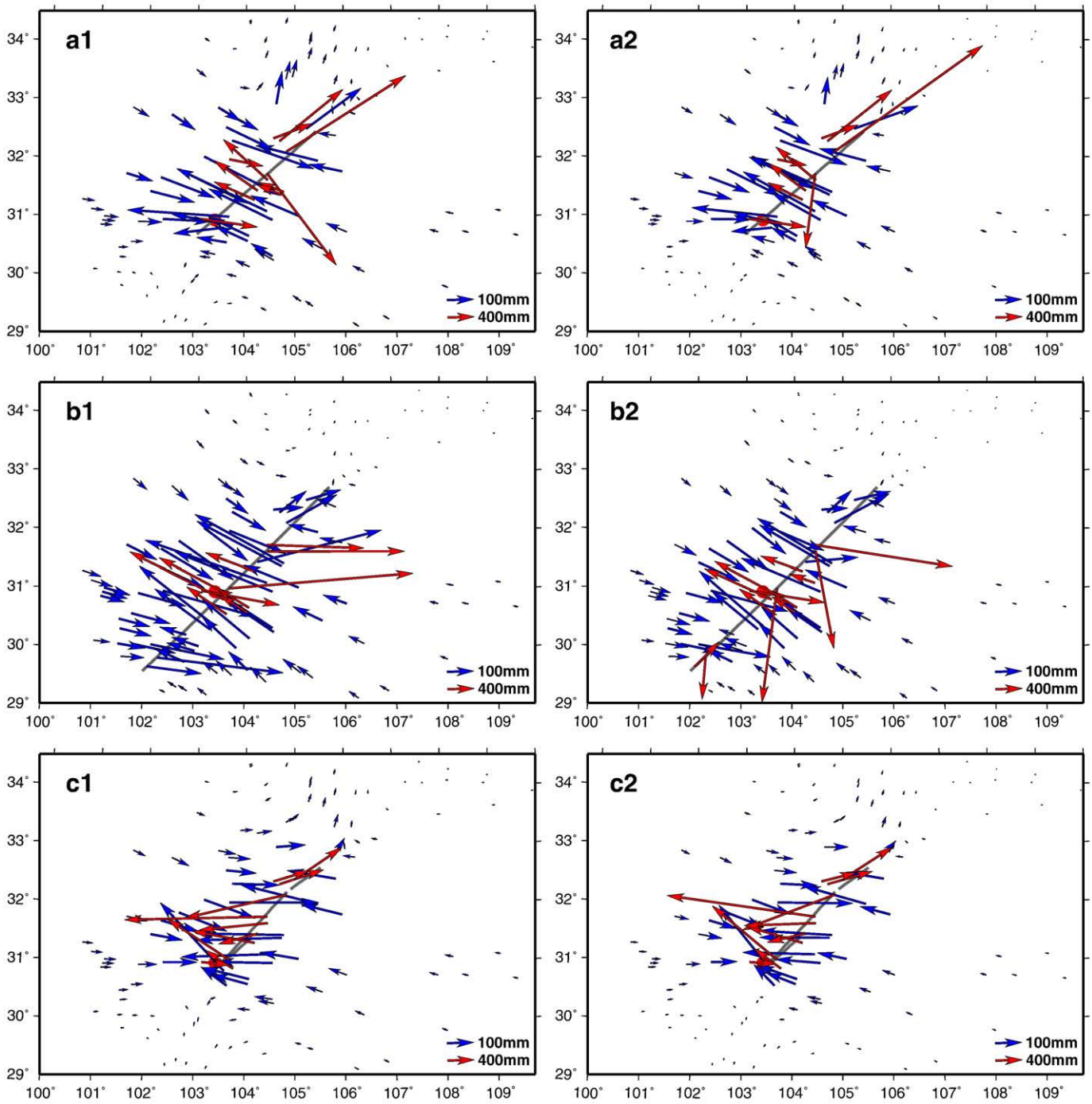

Fig. 4. Calculated co-seismic horizontal displacements caused by the 2008 Wenchuan earthquake (Ms8.0) for three seismic slip models by Ji and Hayes (a_1, a_2; 2008), Zhang et al. (b_1, b_2; 2008a,b) and *Wang et al.* (c_1, c_2; 2008), respectively, using half-space (Okada, 1985; a_1, b_1 and c_1) and spherical (Sun et al. 1996; a_2, b_2 and c_2) dislocation theories for the revised PREM (RPREM) earth model.

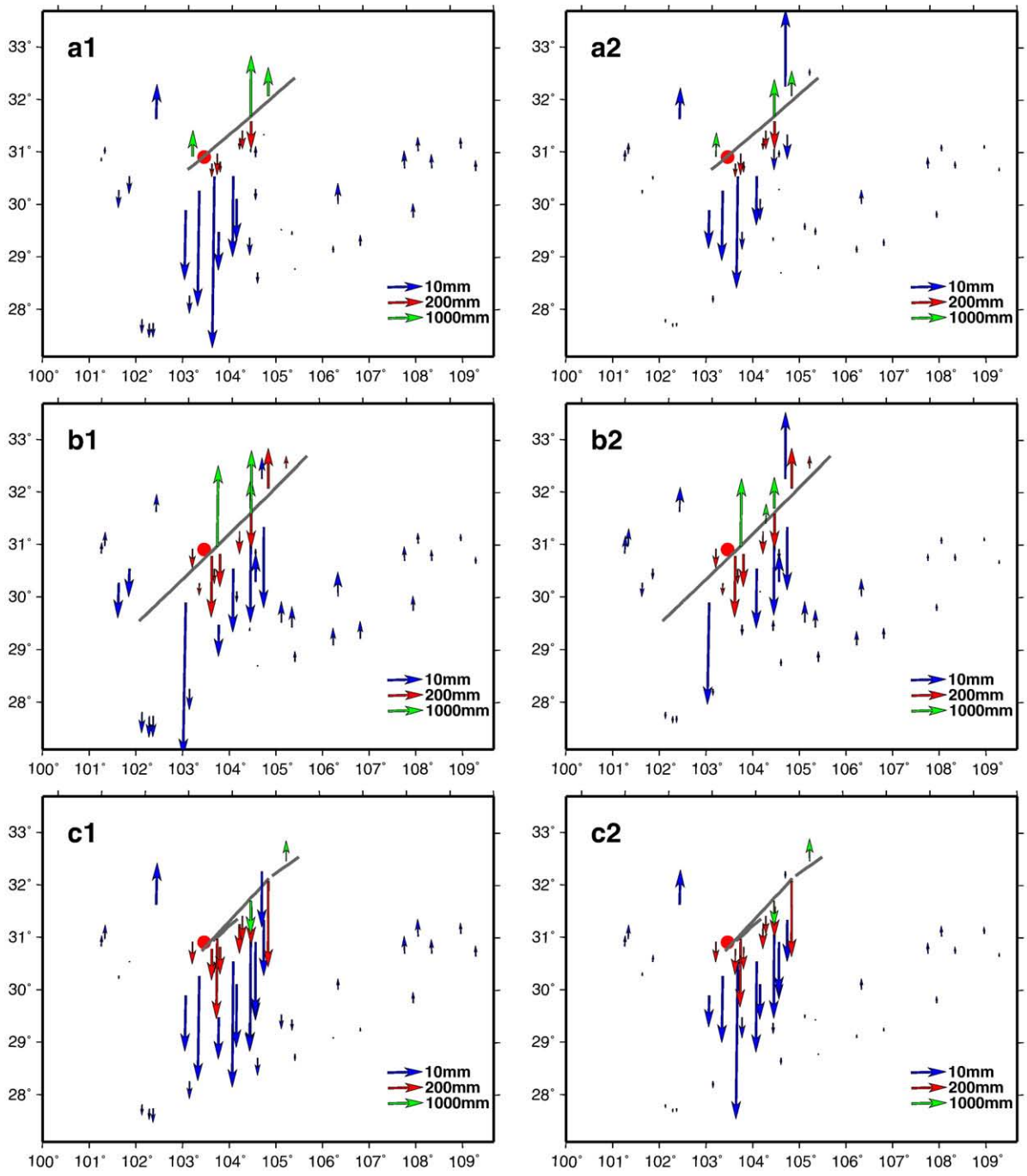

Fig. 5. As shown in Fig. 4, but for vertical displacements.

results in c_2 fit observations best, i.e. the co-seismic displacements calculated using the spherical dislocation theory (Sun et al., 1996, 2009) for the Wang et al. (2008) fault model are the best results to fit the observed ones. To prove this conclusion, we estimate the RMS of these results obtained using the following formula.

$$\hat{\sigma} = \sqrt{\sum_{i=1}^{N} |\mathbf{u}_{obs}^{i} - \mathbf{u}_{cal}^{i}|^2 / n} \quad (1)$$

The numerical RMS results in Table 1 confirm the conclusions presented above. At the same time, the RMS results in Table 1 imply that the effects of the curvature and layered structure of the earth might be readily apparent, and should be considered, especially for

Table 1
RMS comparison between the computed and observed co-seismic displacements.

Fault model	Horizontal displacement				Vertical displacement			
	Half-space theory		Spherical theory		Half-space theory		Spherical theory	
	$\nu=0.33$	$\nu=0.32$	PREM	RPREM	$\nu=0.33$	$\nu=0.32$	PREM	RPREM
Ji and Hayes	51.1	51.1	51.1	48.8	45.3	45.4	36.4	36.4
Zhang et al.	65.4	65.3	59.0	59.1	58.4	58.6	46.8	44.3
Wang et al.	13.8	13.8	13.7	13.1	8.7	9.0	9.1	8.4

Unit: cm.

computing co-seismic deformations attributable to such a large seismic event.

5. Co-seismic deformations caused by the 2008 Wenchuan earthquake (Ms8.0)

According to the discussion presented in the preceding section, the Wang et al. (2008) fault model is far superior to the other two models in fitting the GPS displacements. The spherical dislocation theory (Sun et al., 1996, 2009) yields better results than those obtained from the half-space theory (Okada, 1985). Therefore, in this section, we compute the co-seismic deformations (displacement, geoid, gravity, and strain changes) for the fault model (slip distribution) given by Wang et al. (2008) using the spherical dislocation theory.

The co-seismic displacements are calculated using the formulas presented in Sun et al. (1996, 2009). The results are depicted in Fig. 6, where (a) signifies the EW component, (b) is the NS component, and (c) is the vertical component. The dashed lines in the figures represent the fault line on the earth's surface. Fig. 6 portrays that the co-seismic deformation along the fault line area is complicated. The EW components (a) on both sides of the fault show a strong opposite displacement: the hanging wall moves eastward, about two-times greater distance than that of the foot wall, with a maximum movement of 7 m. The NS component (b) shows a more complicated displacement pattern than that of the EW component. It also indicates that the east fault segment mainly moves northward with a maximum movement of 2.6 m, but the west fault segment mainly moves southward with a maximum movement of about 1 m. The NS component is generally smaller than the EW component. Therefore, the horizontal displacement vector is dominated by the EW component. The displacement pattern in Fig. 6a also exhibits a right-strike-slip component. The vertical displacements (Fig. 6c) show the maximum value along the fault line, up on the hanging wall and down on the foot wall. However, they vary in sign as distance from the fault line increases; they decay rapidly.

Next, we compute the co-seismic geoid and gravity changes using the spherical dislocation theory by Sun and Okubo (1993). Results are depicted in Fig. 7, which show that the geoid rises in the fault zone, reaching 2.1 mm in magnitude. At the same time, the general distribution exhibits a four-quadrant pattern, with positive change in the NS direction and negative in the EW direction. Gravity also shows a four-quadrant pattern, but positive change is apparent in the southern foot wall with the maximum value of 100 μgal; almost negative changes in the hanging wall occur with the maximum value of −650 μgal.

Finally, we calculate the co-seismic strain changes (a, EW; b, NS; c, dilatation; and d, shear components) using the formulas of Sun et al. (2006). Results of the four independent components are depicted in Fig. 8. The unit is 10^{-8} (dimensionless). Similarly, these strain changes exhibit a large magnitude along the fault area. The strain changes from −50,000 to 50,000 nanostrains. Strain is a derivative of displacement. Therefore, they decay rapidly with increased distance from the fault line. The strain results are useful to interpret observed strain changes. They can also be used to compute stress redistribution, like that of Toda et al. (2008). According to Toda et al. (2008), the 2008 Wenchuan earthquake (Ms8.0) was able to trigger additional $M>7$ earthquakes in the Xianshuihe, Kunlun, and Min Jiang faults, about 100–140 km distance from the main shock rupture, where some segments of the stressed faults have not ruptured in more than a century. More detailed investigation of this problem remains as a subject for future study.

6. Co-seismic gravity changes to be detected by GRACE

Finally, it should be pointed out that all the above theories were developed for a deformed earth surface because most traditional measurements are performed on the earth surface. However, advances in modern geodetic techniques, such as the GRACE satellite gravity mission, enable better detection of co-seismic gravity changes from space. For example, the co-seismic and post-seismic gravity changes attributable to the 2004 Sumatra earthquake (M9.3) were detected by GRACE (Gross and Chao, 2001; Sun and Okubo, 2004; Han et al., 2006). In fact, Han et al. (2006) calculated the gravity changes caused by the earthquake, and interpreted the gravity changes using a simple method based on a half-space earth model. Their results show that the magnitude of the gravity change is about ±15 μgal after Gaussian filtering ($R=300$ km) is used. To observe whether or not the co-seismic gravity changes for a smaller earthquake are detectable from space, we calculate the co-seismic gravity changes caused by the 2008 Wenchuan earthquake (Ms8.0). In this case, the gravity changes should be calculated for a space-fixed point instead of the deformed earth surface (Sun et al., 2009). The results are depicted in Fig. 9a. The magnitudes were −100–300 μgal. They indicate large changes along the fault area, as expected.

The GRACE satellite is known to observe only the low-frequency gravity changes because of the attenuation of signals; the accuracy of high-frequency signals is low. In practical applications of satellite data, a filter is usually used for damping the error in the high-frequency part of the signal. For example, Han et al. (2006) adopted a Gaussian filter with a 300 km smoothing radius, which corresponds to the spherical harmonic degree of 60. The same filter is expected to be used in theoretical computation to compare the observed gravity changes with theoretically predicted ones. Then, after applying the Gaussian filter with smoothing radii of 100 and 300 km, the results as shown in Fig. 9b and c show that the gravity varies smoothly. The smoothed gravity changes include only the low-frequency part and become smaller in amplitude, respectively reaching about −1.6–+3.2 μgal for a 100 km filter, and −0.12–+0.24 μgal for a 300 km filter. According to the detection capability of GRACE (Sun and Okubo, 2004), the co-seismic gravity changes seem to be difficult for GRACE to detect. Nevertheless, such changes might be detectable by the GRACE follow-on after it is launched a few years from now. No sufficient released GRACE data are available after the seismic event. Therefore, this conclusion remains to be confirmed later.

7. Summary and remarks

The 2008 Wenchuan earthquake (Ms8.0) was engendered by the collision between the Indian plate and the Eurasian plate. The collision caused an increment of uplift of the mountain range and subsidence of the Sichuan Basin. The two landmasses are moving toward each other, as indicated by the GPS displacements, with one landmass sliding underneath the other. To date, several fault models (slip distribution models) have been proposed. To investigate which model is better in fitting observed geodetic data, we made some comparisons among three selected fault models, two dislocation theories, and two earth models. Results indicate that the combined seismic waveforms and displacement data yield the best fault model. Furthermore, the dislocation theory for a spherical earth model is better than that for a half-space earth model. The modified PREM earth model is better to fit the geodetic data. Based on results described above, co-seismic deformations caused by this earthquake are calculated and discussed, such as displacements, geoid and gravity changes, and strain changes. These results reveal spatial distributions of the crustal deformations, which are useful for inverting seismic faults and studying the interior structure of the earth. They are also expected to serve as references for interpreting the relative geodetic data for other uses. The co-seismic gravity changes observed from space were also calculated and discussed. Finally, it is worth to comment that, the current discussion is based on spherically symmetric earth model (PREM), which is an average 1D homogeneous model and do not represent the lateral heterogeneity of the crust and upper mantle structures. However,

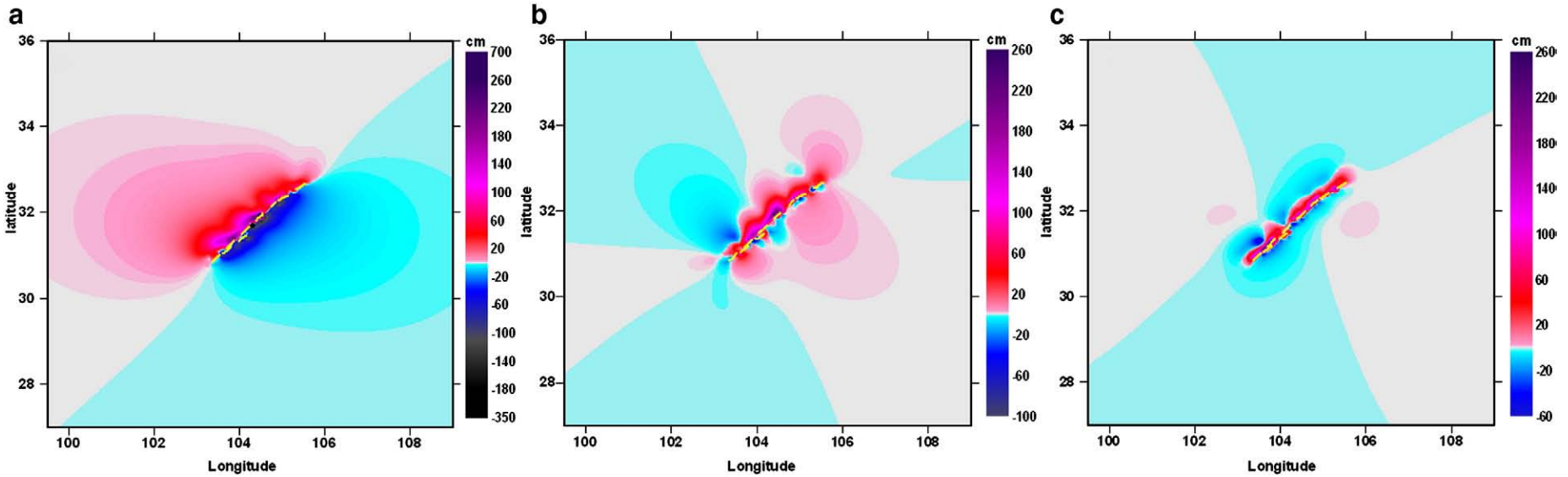

Fig. 6. Distribution of co-seismic horizontal (a = EW, b = NS) and vertical (c) displacements caused by the 2008 Wenchuan earthquake (Ms8.0), as computed using the spherical dislocation theory (Sun et al., 1996, 2009). Positive values in a, b and c are towards the East, North, and up, respectively. Unit: cm.

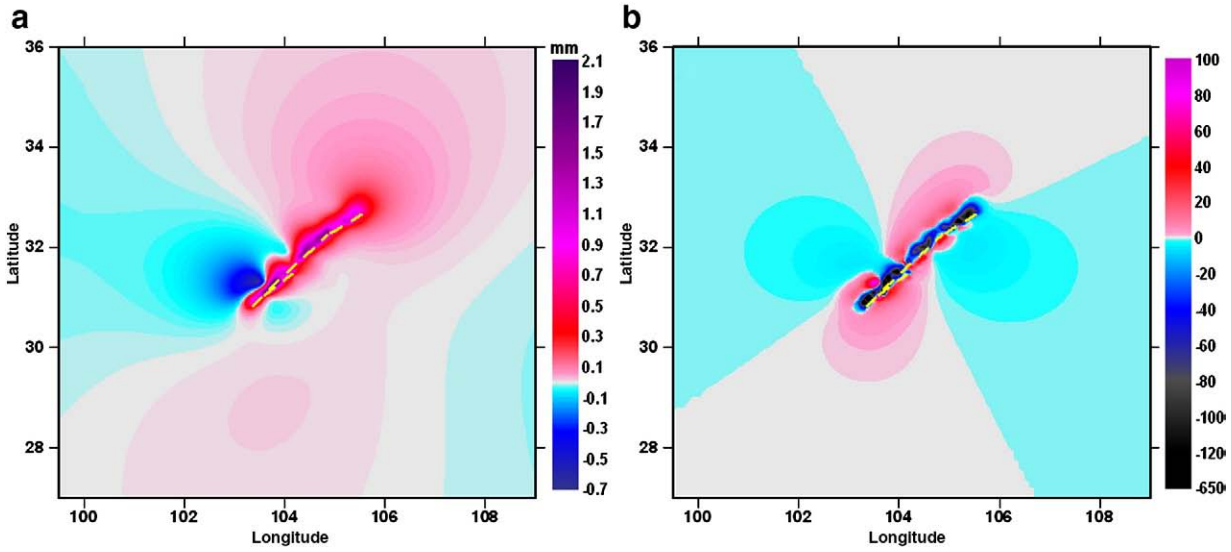

Fig. 7. Distribution of co-seismic geoid (a) and gravity (b) changes caused by the 2008 Wenchuan earthquake (Ms8.0), as computed using the spherical dislocation theory (Sun and Okubo, 1993). Unit: mm for geoid; μgal for gravity.

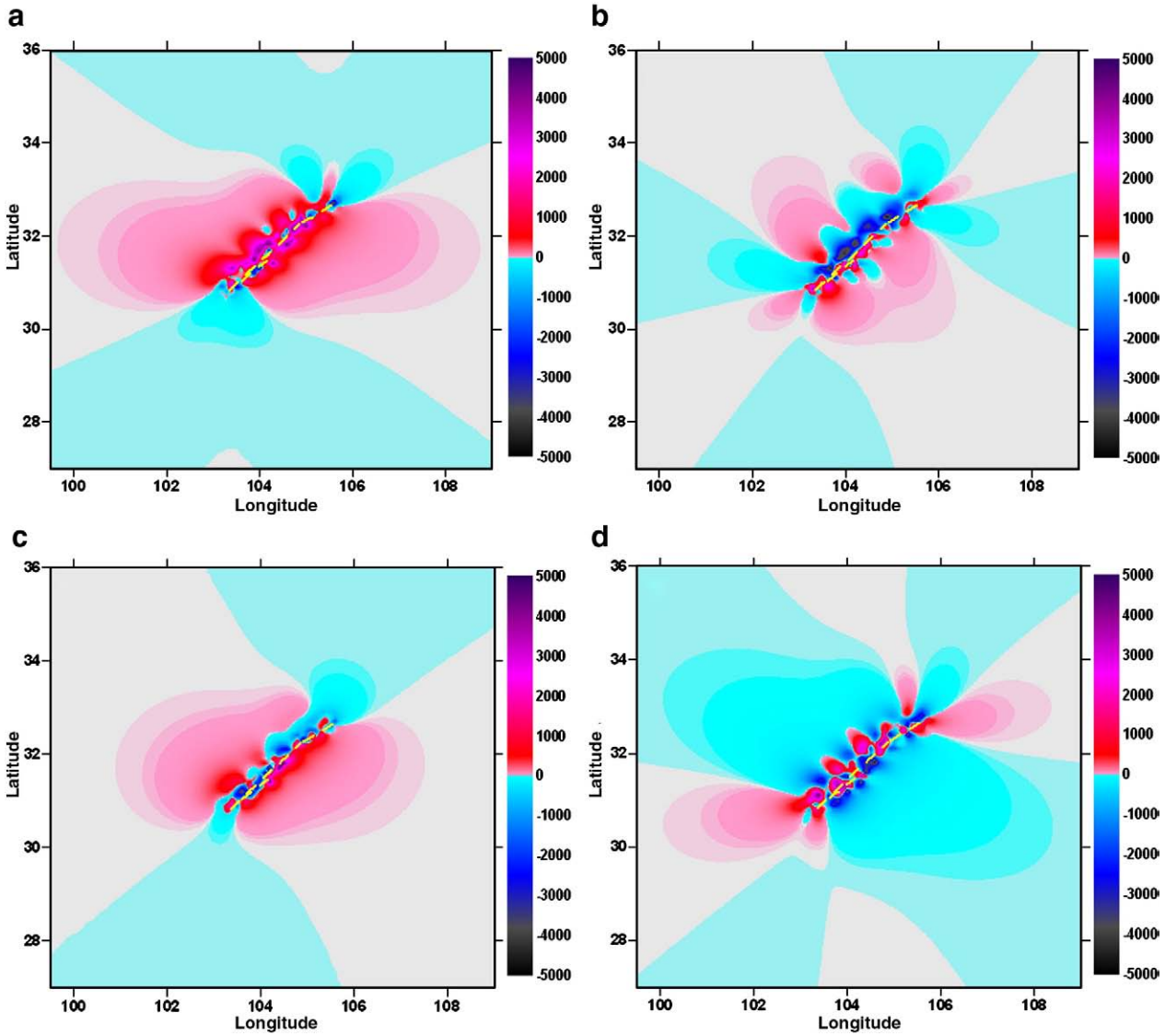

Fig. 8. Distribution of co-seismic strain changes (a, EW; b, NS; c, dilatation; and d, shear components) caused by the 2008 Wenchuan earthquake (Ms8.0), as computed using the spherical dislocation theory (Sun et al., 2006). The unit is 10^{-8}.

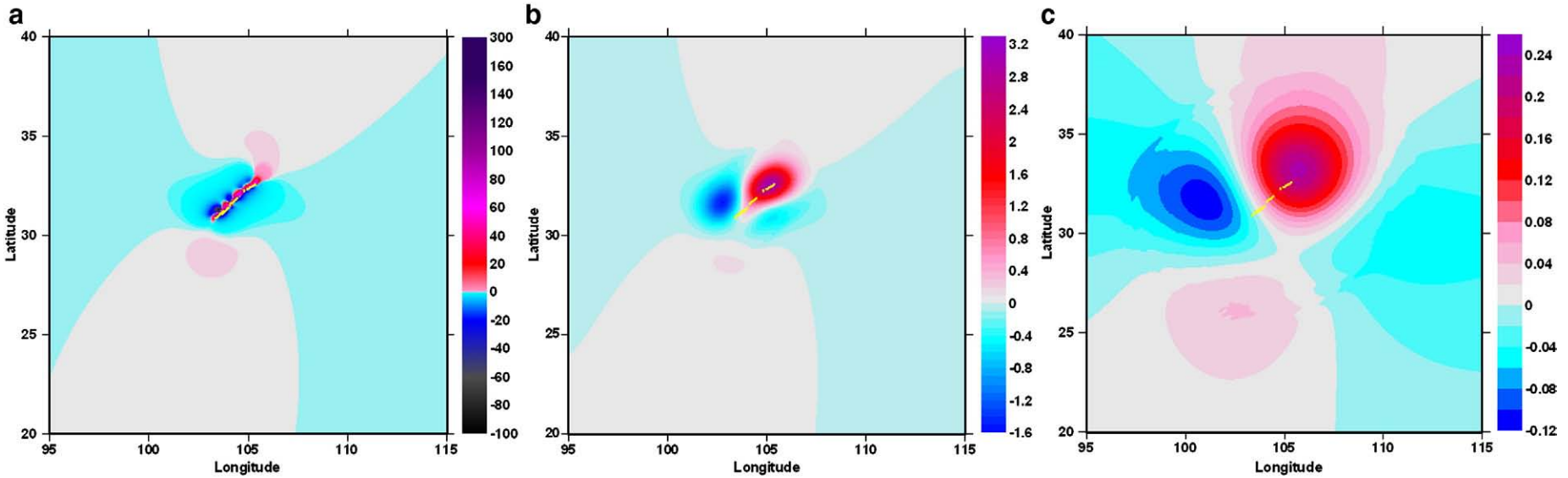

Fig. 9. Co-seismic gravity changes at a space-fixed point (a) with filtered ones by 100 km (b) and 300 km (c) caused by the 2008 Wenchuan earthquake (Ms8.0), computed using the spherical dislocation theory (Sun et al., 2009). Unit: μgal (10^{-8}ms^{-2}).

Longmenshan fault is the boundary of eastern Tibetan Plateau and Sichuan Basin; there is nearly 20 km difference between the crustal thicknesses of the two sides, so the effect of lateral heterogeneity may play important roles on the deformations. An effort to consider the lateral heterogeneity (3D structure) deserves special study in the future.

Acknowledgements

We gratefully acknowledge the supports by the Basic Research Foundation of Institute of Earthquake Science, China Earthquake Administration (Grant No. 02076902-26), and National Key Technologies Research&Development Program of China (Grant No. 2008BAC35B05). And the second author, Wenke Sun, is financially supported by a Grant-in-Aid for Scientific Research from the Ministry of Education, Culture, Sports, Science and Technology, Japan "Comprehensive Investigation on the 2008 Great Earthquake in Sichuan Province and Damage Caused by the Earthquake".

References

Dziewonski, A.M., Anderson, D.L., 1981. Preliminary Reference Earth Model. Phys. Earth Planet. Inter. 25, 297–356.
Fu, G., Sun, W., 2004. Effects of spatial distribution of fault slip on calculating co-seismic displacement: case studies of the Chi–Chi earthquake (Mw7.6) and the Kunlun earthquake (Mw 7.8). Geophys. Res. Lett. 31, L21601. doi:10.1029/2004GL020841.
Fu, G., Sun, W., 2008. Surface co-seismic gravity changes caused by dislocations in a 3-D heterogeneous earth. Geophys. J. Int. 172 (2), 479–503.
Gross, R.S., Chao, B.F., 2001. The gravitational signature of earthquakes. In: Sideris, M.G. (Ed.), Gravity, Geoid, and Geodynamics 2000. IAG Symposia, vol. 123. Springer-Verlag, New York, pp. 205–210.
Han, S.-C., Shum, C.K., Bevis, M., Ji, C., Kuo, C.-Y., 2006. Crustal dilatation observed by GRACE after the 2004 Sumatra–Andaman earthquake. Science 313, 658–662.
Ji, C., Hayes, G., 2008. Preliminary Result of the May 12, 2008 Mw 7.9 Eastern Sichuan, China Earthquake. http://earthquake.usgs.gov/eqcenter/eqinthenews/2008/us2008ryan/finite_fault.php.
Maruyama, T., 1964. Statical elastic dislocations in an infinite and semi-infinite medium. Bull. Earthq. Res. Inst. Univ. Tokyo 42, 289–368.
Okada, Y., 1985. Surface deformation caused by shear and tensile faults in a half-space. Bull. Seismol. Soc. Am. 75 (4), 1135–1154.
Okubo, S., 1991. Potential and gravity changes raised by point dislocations. Geophys. J. Int. 105, 573–586.
Okubo, S., 1992. Potential and gravity changes caused by shear and tensile faults. J. Geophys. Res. 97, 7137–7144.
Piersanti, A., Spada, G., Sabadini, R., Bonafede, M., 1995. Global post-seismic deformation. Geophys. J. Int. 120, 544–566.
Pollitz, F.F., 1997. Gravity anomaly from faulting on a layered spherical earth with application to central Japan. Phys. Earth Planet. Int. 99, 259–271.
Press, F., 1965. Displacements, strains and tilts at teleseismic distances. J. Geophys. Res. 70, 2395–2412.
Sabadini, R., Piersanti, A., Spada, G., 1995. Toroidal/poloidal partitioning of global post-seismic deformation. Geophys. Res. Lett. 21, 985–988.
Steketee, J.A., 1958. On Volterra's dislocations in a semi-infinite elastic medium. Can. J. Phys. 36, 192–205.
Sun, W., Okubo, S., 1993. Surface potential and gravity changes due to internal dislocations in a spherical Earth, 1, Theory for a point dislocation. Geophys. J. Int. 114, 569–592.
Sun, W., Okubo, S., 2002. Effects of the earth's spherical curvature and radial heterogeneity in dislocation studies for a point dislocation. Geophys. Res. Lett. 29 (12), 1605. doi:10.1029/2001GL014497.
Sun, W., Okubo, S., 2004. Co-seismic deformations detectable by satellite gravity missions — a case study of Alaska (1964, 2002) and Hokkaido (2003) earthquakes in the spectral domain. J. Geophys. Res. 109 (B4), B04405. doi:10.1029/2003JB002554.
Sun, W., Okubo, S., Vanicek, P., 1996. Global displacement caused by dislocations in a realistic earth model. J. Geophys. Res. 101, 8561–8577.
Sun, W., Okubo, S., Fu, G., 2006. Green's function of co-seismic strain changes and investigation of effects of Earth's curvature and radial heterogeneity. Geophys. J. Int. 167, 1273–1291. doi:10.1111/j.1365-246X.2006.03089.x.
Sun, W., Okubo, S., Fu, G., Araya, A., 2009. General formulations of global co-seismic deformations caused by an arbitrary dislocation in a spherically symmetric earth model–applicable to deformed earth surface and space-fixed point. Geophys. J. Int. 177, 817–833. doi:10.1111/j.1365-246X.2009.04113.x.
Tanaka, Y., Okuno, J., Okubo, S., 2006. A new method for the computation of global viscoelastic post-seismic deformation in a realistic earth model (I) — vertical displacement and gravity variation. Geophys. J. Int. 164 (2), 273–289.
Toda, S., Lin, J., Meghraoui, M., Stein, R.S., 2008. 12 May 2008 M = 7.9 Wenchuan, China, earthquake calculated to increase failure stress and seismicity rate on three major fault systems. Geophys. Res. Lett. 35, L17305. doi:10.1029/2008GL034903.
Wang, Q., et al., 2001. Present-day crustal deformation in China constrained by global positioning system measurements. Science 294, 574–577.
Wang, W.M., Zhao, L.F., et al., 2008. Rupture process of the Ms8.0 Wenchuan earthquake of Sichuan, China. Chin. J. Geophys. 51 (5), 1403–1410 (in Chinese).
Xu, X.W., Wen, X.Z., Ye, J.Q., et al., 2008. The Ms8.0 Wenchuan earthquake surface ruptures and its seismogenic structure. Seismol. Geol. 30 (3), 597–629 (in Chinese).
Zhang, Y., et al., 2008a. Spatial–temporal rupture process of the 2008 Wenchuan earthquake. Sci. China 38 (10), 1186–1194.
Zhang, P., et al., 2008b. China Crustal Observation Network Project, Co-seismic displacements of the 2008 Wenchuan earthquake (Ms8.0) observed by GPS. Sci. China 38 (10), 1195–1206.